An innovative intermittent hypoxia model for cell cultures allowing fast PO2 oscillations with minimal gas consumption

Mélanie Minoves, Jessica Morand, Frédéric Perriot, Morgane Chatard, Brigitte Gonthier, Emeline Lemarié, Jean-Baptiste Menut, Jan Polak, Jean-Louis Pépin, Diane Godin-Ribuot, et al.

An innovative intermittent hypoxia model in cell cultures allowing fast PO_2 oscillations with minimal gas consumption

Mélanie Minoves[1,2], Jessica Morand[1,2], Frédéric Perriot[1,2], Morgane Chatard[3], Brigitte Gonthier[1,2], Emeline Lemarié[1,2], Jean-Baptiste Menut[4], Jan Polak[5], Jean-Louis Pépin[1,2,6], Diane Godin-Ribuot[1,2], and Anne Briançon-Marjollet[1,2,$]

[1] Univ Grenoble Alpes, HP2 Laboratory, F-38041 Grenoble Cedex, France

[2] INSERM U1042, F-38041 Grenoble Cedex, France

[3] Univ Lyon, UJM-Saint-Etienne, SNA-EPIS, EA4607, F-42023, Saint-Etienne, France

[4] SMTEC, Chemin des Vignes, Nyon, Switzerland

[5] Center for Research on Diabetes, Metabolism and Nutrition Third Faculty of Medicine, Charles University, Prague, Czech Republic

[6] CHU Grenoble, F-38041 Grenoble Cedex, France

[$] **Corresponding author**

Anne Briançon-Marjollet

Laboratoire HP2, Institut Jean Roget

Faculté de Médecine de Grenoble, BP 170

38042 Grenoble Cedex 9, France

Tel: +33 476 63 74 75

Fax: +33 476 63 71 78

E-mail: anne.briancon@univ-grenoble-alpes.fr

Running title: A new cellular intermittent hypoxia model

Abstract

Performing hypoxia-reoxygenation cycles in cell culture with a cycle duration accurately reflecting what occurs in obstructive sleep apnea (OSA) patients is a difficult but crucial technical challenge. Our goal was to develop a novel device to expose multiple cell culture dishes to intermittent hypoxia (IH) cycles relevant to OSA with limited gas consumption.

With gas flows as low as 200 mL/min, our combination of plate holders with gas-permeable cultureware generates rapid normoxia-hypoxia cycles. Cycles alternating 1 minute at 20% O_2 followed by 1 minute at 2% O_2 result in pO_2 values ranging from 124 to 44mmHg. Extending hypoxic and normoxic phases to 10 minutes allows pO_2 variations from 120 to 25mmHg. The volume of culture medium or the presence of cells only modestly affected the pO_2 variations. In contrast, the nadir of the hypoxia phase increased when measured at different heights above the membrane. We validated the physiological relevance of this model by showing that HIF-1α expression was significantly increased by IH exposure in human aortic endothelial cells (HAoEC), murine breast carcinoma (4T1) cells as well as in a blood-brain barrier model (2.5, 1.5 and 6-fold increases, respectively).

In conclusion, we have established a new device to perform rapid intermittent hypoxia cycles in cell cultures, with minimal gas consumption and the possibility to expose several culture dishes simultaneously. This device will allow functional studies of the consequences of IH and deciphering of the molecular biology of IH at the cellular level using oxygen cycles that are clinically relevant to OSA.

INTRODUCTION

Intermittent hypoxia (IH) is the hallmark of obstructive sleep apnea (OSA), a common chronic disease affecting 5-20% of the general population and characterized by recurrent collapses of the upper airway leading to the repetitive occurrence of oxygen desaturation/reoxygenation sequences (14). OSA is recognized as an important and independent risk factor for hypertension, coronary heart disease and stroke, and could also be associated with mild cognitive dysfunction (16). Moreover, recent studies suggest that the excess mortality in OSA could be at least partly due to an increased risk of cancer (5, 19). The molecular pathways underlying the deleterious consequences of OSA are under investigation (8, 10, 26) but cellular and molecular mechanisms remain poorly understood. Moreover, clinical research is limited by confounding factors that make it difficult to distinguish between the respective effects of intermittent hypoxia and comorbidities. Since stroke and coronary heart disease are common OSA-associated comorbidities, increased knowledge of the effects of IH exposure of endothelial cells and blood brain barrier appears to be crucial. Finally, IH is also observed in tumors and exposure of tumor microenvironment to IH might promote tumor growth and metastatic activity (1).

In this context, significant efforts were recently made in several leading laboratories in the field to obtain relevant models of IH in cell cultures. The achievement of rapid oxygen cycles in standard culture dishes is flawed by the very slow oxygen diffusion in culture medium in the absence of mixing (2). Moreover, thermally-induced convective mixing of the media is not sufficient to ensure rapid oxygen equilibration across the height of medium (2, 17, 20) thus limiting the development of relevant IH systems. For instance, one of the first cellular IH model, based on air flushing in a Lucite chamber, generated cycles alternating 15 seconds of 1% O_2 and 3 minutes of 21% O_2 that allowed only limited (between 50 and 70 mmHg) fluctuations in pO_2 in the culture medium (12). This highlights the challenge of oxygen diffusion for effective cell exposure to IH. Longer cycles have allowed cycling between 2% O_2 and 15% O_2, but with cycle durations of one (11) and 1.5 (28) hour, that are not clinically relevant in the context of OSA-related IH. Another strategy has consisted in using pre-equilibrated culture medium (2, 24, 27). In these systems, the use of preconditioned medium does ensure instantaneous oxygen changes at the cell level. However, repeated changes in medium complicate the measurement of soluble factor secretion and can induce an

important shear stress that could impact cell activity and metabolism. More recently, a team has proposed a system in which gas was directly injected in the culture flask (23). They alternated 5 minutes of 16% O_2 and 5 minutes with 0% O_2 resulting in 6 cycles per hour which was the best compromise to achieve sufficient oxygen variation amplitude.

Finally, the last type of system described in the literature uses gas permeable dishes in order to obtain rapid and accurate cycles at the cell level (18, 22). In this system, variations between 16% and 1% O_2 lead to similar oxygen variations in the culture medium within minutes, allowing a frequency of 6 cycles per hour without any change in medium or bubbling. The major disadvantage of this elegant setting is the high gas consumption necessary to replace the air volume of the cabinet incubator hosting the dishes. Achievement of the control normoxic exposure also relies on expensive pre-mixed gas bottles (16% O_2, 5% CO_2 and 79% N_2). Recently, a variant of this system, based on air circulation underneath highly-permeable PDMS (polydimethylsiloxane) membranes for cell culture, achieved very fast oxygen cycles at the cell level in a system adapted for direct microscopy imaging (4). The major limitation of this model relies on its small size (4-mm diameter dishes) and thus in the low number of exposed cells, preventing large scale studies or the collection of cells for biochemical or molecular biology studies.

Therefore, our objective was to set up a cost-effective and rapid-cycling model producing IH cycles able to mimic the tissue oxygenation characteristics of OSA. We aimed at developing and characterizing a device that would allow rapid oxygen cycling, minimal gas consumption, avoiding the use of expensive premixed gas bottles, and allowing exposure of multiwell plates and larger culture plates. The originality of this system is that it generates rapid cycles in culture media while minimizing gas consumption by using gas-permeable cell cultureware and custom made holders in which the air is renewed only below the dishes.

MATERIALS AND METHODS

Gas-permeable dishes and plate holders.

Gas-permeable dishes were either from Sarstedt (Lumox® 55-mm dishes, 24- and 96-well plates, Sarstedt, Germany) or from Zell-Kontakt (Fluorocarbon Imaging plates, 24- and 96-

well plates, Zell-Kontakt GmbH, Germany). The thickness of the membrane is 25 µm for Zell-Kontakt plates and Sarstedt dishes, while it is 50 µm for Sarstedt plates. Since poor cell adhesion was observed with both types of membranes, they were coated with type I collagen (0.2 mg/ml for 1 h at 37°C) before seeding cells.

Transwells with either 0.4 µm or 8 µm pores (Corning) were placed in 24-well Zell-Kontakt plates. Transwells and plate wells were filled with 200 µL and 600 µL of culture medium, respectively.

The plate holders were custom-made (SMTEC, Nyon, Switzerland) to accommodate either 55-mm dishes or 24- or 96-well plates (Figure 1). The dishes or plates are attached to the holders with clips in order to minimize air leakage. The air volume under the plate or dish is as low as 15-20 ml thus allowing very rapid flushing, even with flows as low as 200 ml/min, and very low gas consumption.

Gas supply.

Compressed air and >98% nitrogen are provided by a nitrogen extractor and a gas compressor and carbon dioxide is supplied by a gas bottle. The three gas inputs are connected to a gas blender (Gas Blender 100, MCQ Instruments, Rome, Italy) that can mix gases in any desired fraction with a maximum output flow of 250 ml/minute. The gas mixture is heated in a water bath set a 37°C and travels through a 5-meter long plastic tube to allow temperature equilibration before being transmitted to culture plate holders hosted in a standard cell culture incubator. Pressure equilibration is possible with air above the culture medium, thus the system operates under normobaric conditions

Oxygen measurements.

Oxygen in air was measured with a gas analyzer (ADInstruments, Oxford, United Kingdom). Dissolved oxygen in culture medium was measured with pre-calibrated fluorescent oxygen sensors (pO_2 E-Series Sensor) coupled to an Oxylite device (Oxford Optronix, Oxford, United Kingdom). The sensors have a 90% response time of 20 seconds and a precision of 0.1 mmHg. The pO_2 sensors were maintained by a holder equipped with a micrometer screw and a binocular microcope, allowing the direct observation of the contact between the probe and the membrane, and the vertical movement of the sensor by 60-µm steps from the

membrane level (pericellular environment) up to the top of the culture medium. In sealed dishes, the probe was inserted through a needle hole in the lid before sealing. Data were recorded using an acquisition system (Powerlab, ADInstruments, Oxford, United Kingdom).

Experimental intermittent hypoxia protocols.

Different pO_2 cycling protocols were programmed to characterize the behavior of the model (Table 1). The IH protocols alternated a 20% or 16% normoxic phase and a 5% or 2% hypoxic phase. The 16% oxygen value of normoxic phase was chosen according to the mean arterial pO_2 value of healthy humans, as in other IH models (22, 23). We programmed IH protocols with 5% (5% 2'-2' and 3'-3') and 2% (2% 30"-30", 1'-1', 2'-2', 3'-3', 3'-5' and 5'-5') hypoxic phases named according to the duration (in seconds or minutes) of the normoxic and hypoxic phases, respectively. Following hypoxia, a brief 20% O_2 phase was used to accelerate the return towards the normoxic 16% plateau. Similarly, a 1-minute burst of 3% pO2 was added to rapidly attain a stable 5% hypoxic plateau. No burst was used to attain the 2% hypoxic plateau, since 2% is the minimum oxygen contain of our gas supply (98% pure nitrogen). Carbon dioxide was always set at 5% in the gas mixture.

Cell culture and HIF-1α quantification.

Human aortic endothelial cells (HAoEC, Cascade Biologics) were cultured in M200 medium, supplemented with large vessel endothelial supplement (LVES) as recommended by the manufacturer, and used after 6-8 population doubling. Human breast carcinoma cells (4T1, graciously provided by V. Josserand, IAB, Grenoble) were cultured in RPMI medium supplemented with 10% fetal bovine serum and antibiotics. The blood-brain barrier (BBB) model is composed of bEnd.3 endothelial cells (ATCC, USA) combined to C6 astrocytes (ATCC, USA) cultured in transwells with 0.4µm pores, as previously described (6).

HAoEC and 4T1 cells were exposed to 6 hours of IH (protocol 2% 5'-5'). BBB model was exposed to 2h of IH (protocol 2% 5'-5') followed by 6 hours of normoxia (16% O_2), repeated 3 times for a total of 24 hours.

At the end of IH exposure, supernatants were collected and frozen (-80°C), while the cells were fixed in 4% paraformaldehyde (PFA) for 10 minutes and kept at 4°C until use. HIF-1α expression was measured with a cell-based Elisa assay (R&D Systems) on PFA-fixed cells.

Statistical analysis.

Data were analyzed using GraphPad Prism 6 Software (San Diego, California). The various statistical tests performed are detailed in figure legends. Normality was determined using D'Agostino-Pearson normality tests as recommended by the GraphPad Prism software. Normal data were expressed as means ± SEM. Statistical significance was set at $P < 0.05$.

RESULTS

Rapid intermittent hypoxia cycles with appropriate amplitude were achieved with the model.

Fig. 2 and Table 2 depict typical oxygen cycles observed in 55-mm dishes, filled with 5 ml of PBS, with the various protocols tested (see Table 1 for details of gas settings).

Short cycles composed of 30 seconds at 20% followed by 30 seconds at 2% resulted in oxygen cycling between 105.8 ± 1.3 and 58.5 ± 2.2 mmHg in the culture medium (Fig. 2*A*). Increasing the duration of the normoxic and hypoxic phases enhanced the nadir-to-peak amplitude, with cycles between 124.3 ± 2.4 and 44.3 ± 1.5 mmHg (nadir-to-peak amplitude: 79.9 ± 3.6 mmHg) with protocol 2% 1'-1' (Fig. 2*B*), and between 118.8 ± 2.4 and 33.8 ± 0.3 mmHg (nadir-to-peak amplitude: 84.4 ± 1.9 mmHg) with protocol 2% 2'-2' (Fig. 2*C*). Protocols with a 2-min normoxic phase resulted in a pO_2 plateau around 120 mmHg and pO_2 values > 110 mmHg were achieved within a mean time of 52.1 ± 2.2 seconds. Protocols with 5% O_2 generated a hypoxic plateau around 40 mmHg (Fig. 2*D* and Table 2). For protocols with 2% O_2, a hypoxic plateau was more difficult to achieve, even with a 5-minute hypoxia duration (Fig. 2*E* and 2*F*) and time to reach pO_2 values < 50 mmHg and < 40 mmHg was 47.2 ± 4.5 and 89.0 ± 9.1 seconds, respectively. pO_2 values < 30 mmHg were reached after 3 minutes of hypoxia with protocols 2% 3'-3' and 2% 5'-5' while the minimum value of 25 mmHg could only be attained after 5 minutes of hypoxia (Fig. 2*F*, 2*G* and Table 2). On the other hand, decreasing the duration of normoxia from 5 to 3 minutes resulted in identical peak and nadir pO_2 values (Fig. 2*F* and Table 2).

Since our 55-mm dish holder is designed for 3 dishes, we measured the cycles in the 3 dishes and did not observe any difference in cycle pattern or pO_2 range (Fig. 2*H*).

Effects of cultureware type and membrane thickness on intermittent hypoxia cycles.

We compared the impact of support type and membrane thickness on the nadir-to-peak amplitude of the cycles generated by protocols 2% 3'-3' and 2% 5'-5'. Whatever the protocol, we did not observe any difference on nadir-to-peak cycle amplitude between 25 µm-thick 24-well or 96-well plates and 55-mm dishes. Hence, typical cycles generated by protocol 2% 5'-5' in 24-well plates were between 26 and 113 mmHg (Fig. 3*A*), similar to those observed in 96-well plates and 55-mm dishes. We serially connected three 96-well plates in order to compare the typical aspect of the pO_2 cycles. We did not observe a difference in pO_2 cycles between the three plates (Fig. 3*B*).

However, there was a significant difference in nadir values and nadir-to-peak amplitude of the cycles measured in 25 µm-thick and 50 µm-thick 24-well plates (Fig. 3*C*). Hence, nadir values were significantly lower in 25 µm-thick plates compared to 50 µm-thick plates (27.0 ± 1.9 vs. 55.4 ± 2.3 mmHg, respectively, $P = 0.008$) while peak pO_2 values were not affected (118.6 and 114.6 mmHg, respectively). Therefore, nadir-to-peak amplitude was 91.8 ± 2.9 mmHg in 25 µm-thick plates but only 59.2 ± 2.9 mmHg in 50 µm-thick plates ($P = 0.008$).

Culture medium volume modestly alters the intermittent hypoxia cycles.

Overall, culture medium volume had a significant impact on the cycles ($P = 0.037$) (Table 3). In particular, the lowest nadir value was obtained with a volume of 5 ml (27.2 ± 2.4 mmHg vs. 36.7 ± 2.9 mmHg with a 3 ml volume, $P = 0.019$). However, the nadir-to-peak amplitude was not significantly affected by culture medium volume (101.3 ± 2.9, 103.2 ± 1.6 and 104.7 ± 0.3 mmHg for 3, 5 and 7 ml, respectively).

Presence of cells decreases the amplitude of intermittent hypoxia cycles.

The presence of cells induced a significant decrease in the nadir-to-peak amplitude of the IH cycles (from 95.6 ± 3.0 to 86.5 ± 1.5 mmHg, $P = 0.004$) (Table 4). More precisely, the

presence of cells decreased the maximum pO_2 value (from 124.4 ± 0.9 to 113.1 ± 3.5 mmHg, $P < 0.01$) without affecting the minimum value.

Amplitude of intermittent hypoxia cycles decreases from bottom to top of culture medium.

To test the homogeneity of the cycles throughout the culture medium, we recorded oxygen cycles from the membrane up to the top of the liquid layer using protocols 2% 3'-3' and 2% 5'-5'. To estimate the effect of gas exchange with ambient air we also measured pO_2 gradient with protocol 2% 5'-5' in dishes sealed with tape. Whatever the distance from the membrane and the IH protocol, the maximum pO_2 value remained stable. However, as expected, the minimum pO_2 value linearly increased when the O_2 probe was moved away from the membrane and the nadir-to-peak amplitude therefore concomitantly decreased (Fig. 4*A*). Moreover, AUC obtained with sealed-plates was significantly higher than that recorded in unsealed plates ($P = 0.012$) (Fig. 4*B*).

Finally, to evaluate the possibility of using transwells for co-cultures or for permeability or migration assays under IH, we measured cycles in transwell inserts placed in 24-well permeable plates. The nadir-to-peak amplitude of IH cycles measured in transwells increased with pore diameter. Indeed, amplitudes of 49 mmHg (nadir and peak pO_2 values of 78 and 127 mmHg) and 59 mmHg (nadir and peak pO_2 values of 66 and 125 mmHg values) (Fig. 4*C*) were measured in transwells with 0.4 µm and 8 µm pores, respectively.

Gas permeable dishes allow optimal cell oxygenation under normoxic conditions.

Baseline culture medium pO_2 values measured in plastic dishes with 4T1 cells were significantly lower than those measured in permeable dishes independently of cell confluence (Fig. 5). At 70% confluence, median pO_2 values of 120 and 137 mmHg were measured in plastic and permeable dishes, respectively ($P = 0.016$). At 100% confluence, median pO_2 values of 115 and 150 mmHg were measured in plastic and permeable dishes, respectively ($P = 0.008$). Interestingly, no difference between plastic and permeable dishes was observed with 100% confluent HAoEC cells.

Intermittent hypoxia exposure increases HIF-1α expression in cells.

Six hours of cell exposure to IH with protocol 2% 5'-5' resulted in a significant increase in HIF-1α expression compared to normoxia (2.4 and 1.4 fold-increase in HAEC and 4T1 cells, respectively, $P < 0.05$) (Fig. 6*A*).

Moreover, repeated IH exposure over 24h of a cell BBB model resulted in a very significant increase in HIF-1α expression compared to normoxia (6.1 fold-increase, $P < 0.01$) (Fig. 6*B*).

DISCUSSION

In this paper, we describe an innovative system aiming to perform exposure of cells cultures to intermittent hypoxia with a pattern accurately mimicking that occurring in sleep apnea patients. This system is adapted from commercial gas-permeable dishes and uses custom-made plate holders. The small volume of air in the holders is easily renewed even with low gas flow, thus allowing low gas consumption and fast cycling. Our system is working with gas sources (air, CO_2 and N_2) either from commercial bottles (CO_2) or produced by gas extractor and compressor, thus avoiding expensive premixed gas bottles described elsewhere (22). We were able to connect up to 3 holders in series, thus allowing the simultaneous exposure of three multiwell plates (24-well or 96-well) or up to nine 55-mm dishes, or combinations of multiwell plates and 55-mm dishes. This low cost system effectively produced short IH cycles in culture medium and allowed the exposure of a large number of cells. This should help the field to address molecular biology of IH exposure with a relevant physiological model.

We characterized the oxygen cycles obtained with various settings, with normoxic phases between 20 and 12% oxygen and hypoxic phases between 5% and 2%. With 16%-2% cycling at a frequency of 6 to 8 cycles per hour, we obtained nadir-to-peak amplitudes of about 95 mmHg, cycling between 25-30 mmHg and 120 mmHg. Although a nadir value of 25-30 mmHg is not as low as those attained with other systems (4, 23), it is relevant to OSA physiopathology since 30 mmHg roughly corresponds to the lowest arterial blood saturation level (60% oxygen saturation) recorded in severe sleep apnea patients during hypoxic episodes (15). Similarly, the peak can be chosen at any value up to 125 mmHg, which was

chosen to be slightly higher than the mean value of arterial pO_2 in healthy humans, as done in other IH models (22, 23). Therefore, our system can reproduce patterns of hypoxia-reoxygenation relevant to severe human OSA by cycling between 30 and 100-120mmHg or to moderate OSA by cycling between 40-45mmHg and 100-120mmHg. This is a major advantage to appropriately assess the dose-response relationship between the amount of IH and its deleterious or preconditioning outcomes (13, 14).

Although similar cycles were observed in Lumox® dishes and in fluorocarbon plates which have 25µm-thick membranes, cycles measured in plates with 50µm-thick Lumox® membranes presented high nadir values and decreased nadir-to-peak amplitudes. This suggests that Lumox® membrane thickness can affect gas diffusion. In contrast, similar cycles were recorded with 10µm- and 37.5µm- thick PDMS membranes in another IH system (4). This discrepancy could be due to different chemical composition and/or thickness of the membranes.

Uncoated gas-permeable membranes result in poor cell adhesion and were recently shown to profoundly affect cell morphology and function (21). We thus established that fibronectin, collagen or Matrigel® coating did not significantly alter the cycles measured in the culture medium (data not shown). We also observed that the presence of cells modestly decreased peak values and amplitude of the cycles, whereas nadir values were unchanged. The difference in cycles in the presence of cells could be due to oxygen consumption and/or to impaired gas diffusion through the cell layer. Nevertheless, since the impact of the presence of cells was modest (<10% decrease in cycle amplitude), we can conclude that the membrane maintains good gas permeability even in the presence of a confluent cell monolayer.

Variations in culture medium volume also modestly affected the IH cycles. While peak values and nadir-to-peak amplitude were not significantly altered, nadir values measured in 55-mm dishes were lower at high (5mL) compared to low (3mL) medium volume. This could be explained by oxygen retrodiffusion from air above the medium since low volumes result in thin thickness (approximately 1 mm with 3ml vs. 2 mm with 5ml in 55-mm dishes). Thus, it appears mandatory to always use the same amount of culture medium in order to ensure reproducibility of the IH cycles.

A drawback of some IH systems is the limited number of dishes or plates that can be exposed simultaneously, resulting in insufficient amount of cells for biochemical analysis or molecular biology. In order to minimize gas consumption, we did not choose to perform IH cycles directly in the cell incubator as in other systems (22), but we wanted to be able to expose at least several 55-mm dishes or multiwell plates. Our use of custom-designed plate holders branched in series enabled us to obtain similar cycles in up to 3 multiwell plates or nine 55-mm dishes (or combinations of multiwell plates and 55-mm dishes) simultaneously exposed to IH. This setup ensures that several experiments can be performed simultaneously and that a sufficient quantity of cells can be collected for biochemical analysis or molecular biology.

However, since gases are diffusing from below the plate, we expected that the cycles would perform well at the membrane level only. This is perfectly suitable for adherent cells but represents a limitation for non-adherent cell cultures, such as monocytes or PBMC, or for co-culture systems such as transwell inserts. Indeed, while the peak value was unchanged, we observed that the nadir of the IH cycles gradually increased when measured away from the membrane so that the cycles almost disappeared at the top of the liquid layer. However, adequate IH cycles oscillating between 50 and 110 mmHg were still measured 500 µm above the membrane. Moreover, cycles measured inside 8 µm-pore transwells, commonly used for cell migration or permeability assays, oscillated between 65 and 125 mmHg, suggesting that our system can be used to study the effects of moderate IH on cell migration. Furthermore, our system was successfully used to induce a clear increase of HIF-1 expression in cells cultured in 0.4µm-pore transwell.

Indeed, HIF-1α expression was increased by more than 6 fold in a BBB model composed of endothelial cells and astrocytes cultured in transwells and exposed to IH. In addition to transwells, we observed that HIF-1α expression was increased by 2.6 and 1.5 fold, in primary endothelial and in tumor cells, respectively, after 6h of IH exposure. It should be stressed that HIF-1α expression might have been underestimated in our experimental conditions since it was assessed in PFA-fixed samples, in which PFA could have interfered with antigen reactivity. In accordance with various other studies, we chose to use HIF-1α expression as a marker of hypoxia sensing to validate IH exposure of our cells. Hence, Yuan et al. reported an increase in HIF-1 protein level in nuclear extracts together with an increase in HIF-1 reporter

genes in PC12 cells after 60 cycles of IH (4min-30sec, 20%-1.5%) (31), and more recently Campillo et al. observed a 1.5 fold increase in HIF-1α nuclear translocation in mesenchymal stem cells exposed to 4h of IH (30sec-30sec, 20%-1%) (4). In a very different system, exposure of endothelial cells to long IH cycles (1h-30 min, 20%-1%,) did not increase HIF-1 gene expression but increased its nuclear translocation and DNA binding activity (29). Nevertheless, other studies have failed to observe changes in HIF-1 expression or transcriptional activity with different paradigms of IH exposure (22-24). Thus, despite numerous studies in animal models showing that HIF-1 is activated by intermittent hypoxia in various organs (3, 7, 30), the determinants of HIF-1 activation in cells exposed to IH remain to be assessed, with particular emphasis on the characteristics of the IH cycles (minimal and maximal pO_2, duration of normoxic and hypoxic phases, total duration of exposure or number of cycles) and on the metabolic activity of the cells exposed.

Finally, we compared standard plastic dishes and permeable dishes under normoxic condition. We measured a difference of up to 50 mmHg between standard plastic and semi-permeable dishes, depending on cell type and confluence rate. Indeed the biggest difference was observed for metabolically active cancer cells. These results are consistent with previous data showing different levels of culture medium hypoxia with more or less metabolically active cells (17, 22). In particular, Polak et al. showed that HIF-1 activity was much higher in standard than in permeable plates, probably due to poor oxygenation of culture medium in plastic plates along with O_2 consumption by cells (22). Despite the fact that oxygen tension during standard cell culture if often a neglected factor, these results suggest that it could be of interest to use gas permeable plates even in routine use under normoxic conditions, in order to ensure real and reproducible normoxia at different stages of cell culture and confluence levels.

It should be pointed that the pO_2 measurements performed in the present study were recorded with probes having a 90% response time of 20 seconds (data provided by the manufacturer and experimentally verified in our lab, data not shown), which is not negligible compared to the rise and decay duration of our IH cycles. Therefore, one can assume that the oxygen cycles performed by our system are actually faster than those measured and that the rise and decay durations are overestimated. Moreover, pO_2 values measured for short cycles that did not reach plateau values might be inaccurate so that the nadir-to-peak

amplitude might actually be larger than reported. Nevertheless, we can suggest that the peak and nadir pO_2 values measured for longer IH cycles (3'-3' or 5'-5') were estimated with a good accuracy since we were able to attain plateau phases at in both cases. Carbon dioxide was set at 5% in all gas mixtures, and since CO2 has a very high diffusion coefficient it was theoretically stable in the culture medium throughout intermittent hypoxia exposure.

In summary, we have developed a new low-cost device to perform rapid intermittent hypoxia cycles at the cellular level characterized by very low gas consumption and good cell throughput for biochemistry or molecular biology analysis. This device can be used to mimick the cellular impact of OSA but also that of other pathological conditions in which rapid hypoxia-reoxygenation cycles are observed, such as ischemia-reperfusion events in heart, brain or other organs, or tumor development where oxygen variations can be observed independently of OSA, due to structural abnormalities of the vascular network (9, 25). This device thus presents a new alternative to existing techniques for laboratories that plan to perform cellular IH or simply want to precisely control oxygen tension in their cell cultures.

GRANTS

This work was funded by INSERM, University Grenoble Alpes and Agir pour les Maladies Chroniques (APMC) foundation. It was also partly supported by the French National Research Agency in the framework of the "Investissements d'avenir" program (ANR-15-IDEX-02).

DISCLOSURES

No conflicts of interest, financial or otherwise, are declared by the author(s).

AUTHOR CONTRIBUTIONS

M.M., J.P., D.G-R. and A.B-M. conceived and designed the model; M.M., J.M., F.P., M.C., B.G., E.L., J-B.M. and A.B-M. performed experiments, analyzed data and interpreted results of experiments; A.B-M. and M.M. prepared figures; M.M., J.M., and A.B-M. drafted

manuscript; J.P., J-L.P. and D.G-R. edited and revised manuscript; all authors approved the final version of the manuscript.

ACKNOWLEDGEMENTS

We are grateful to Emmanuel Barbier and Benjamin Lemasson (Grenoble Institute of Neurosciences) for sharing the Oxylite device and to Véronique Josserand (Institute for Advanced Biosciences, Grenoble) for kindly providing the 4T1 cells. We also would like to thank Mathis Soubeyrand and Alexandre Frémont for their technical assistance.

REFERENCES

1. Almendros I, Montserrat JM, Torres M, Dalmases M, Cabanas ML, Campos-Rodriguez F, Navajas D, and Farre R**.** Intermittent hypoxia increases melanoma metastasis to the lung in a mouse model of sleep apnea. *Respir Physiol Neurobiol* **186**: 303-307, 2013.
2. Baumgardner JE and Otto CM**.** In vitro intermittent hypoxia: challenges for creating hypoxia in cell culture. *Respir Physiol Neurobiol* **136**: 131-139, 2003.
3. Belaidi E, Joyeux-Faure M, Ribuot C, Launois SH, Levy P, and Godin-Ribuot D**.** Major role for hypoxia inducible factor-1 and the endothelin system in promoting myocardial infarction and hypertension in an animal model of obstructive sleep apnea. *J Am Coll Cardiol* **53**: 1309-1317, 2009.
4. Campillo N, Jorba I, Schaedel L, Casals B, Gozal D, Farre R, Almendros I, and Navajas D**.** A Novel Chip for Cyclic Stretch and Intermittent Hypoxia Cell Exposures Mimicking Obstructive Sleep Apnea. *Front Physiol* **7**: 319, 2016.
5. Campos-Rodriguez F, Martinez-Garcia MA, Martinez M, Duran-Cantolla J, Pena Mde L, Masdeu MJ, Gonzalez M, Campo F, Gallego I, Marin JM, Barbe F, Montserrat JM, and Farre R**.** Association between obstructive sleep apnea and cancer incidence in a large multicenter Spanish cohort. *Am J Respir Crit Care Med* **187**: 99-105, 2013.
6. Chatard M, Puech C, Roche F, and Perek N**.** Hypoxic Stress Induced by Hydralazine Leads to a Loss of Blood-Brain Barrier Integrity and an Increase in Efflux Transporter Activity. *PLoS One* **11**: e0158010, 2016.
7. da Rosa DP, Forgiarini LF, Baronio D, Feijo CA, Martinez D, and Marroni NP**.** Simulating sleep apnea by exposure to intermittent hypoxia induces inflammation in the lung and liver. *Mediators of inflammation* **2012**: 879419, 2012.
8. Dematteis M, Godin-Ribuot D, Arnaud C, Ribuot C, Stanke-Labesque F, Pepin JL, and Levy P**.** Cardiovascular consequences of sleep-disordered breathing: contribution of animal models to understanding the human disease. *ILAR journal / National Research Council, Institute of Laboratory Animal Resources* **50**: 262-281, 2009.
9. Dewhirst MW, Braun RD, and Lanzen JL**.** Temporal changes in PO2 of R3230AC tumors in Fischer-344 rats. *Int J Radiat Oncol Biol Phys* **42**: 723-726, 1998.
10. Drager LF, Jun JC, and Polotsky VY**.** Metabolic consequences of intermittent hypoxia: relevance to obstructive sleep apnea. *Best Pract Res Clin Endocrinol Metab* **24**: 843-851, 2010.
11. Dyugovskaya L, Polyakov A, Lavie P, and Lavie L**.** Delayed neutrophil apoptosis in patients with sleep apnea. *Am J Respir Crit Care Med* **177**: 544-554, 2008.
12. Kumar GK, Kim DK, Lee MS, Ramachandran R, and Prabhakar NR**.** Activation of tyrosine hydroxylase by intermittent hypoxia: involvement of serine phosphorylation. *J Appl Physiol (1985)* **95**: 536-544, 2003.

13. Lavie L. Oxidative stress in obstructive sleep apnea and intermittent hypoxia--revisited--the bad ugly and good: implications to the heart and brain. *Sleep Med Rev* **20**: 27-45, 2015.
14. Levy P, Kohler M, McNicholas WT, Barbe F, McEvoy RD, Somers VK, Lavie L, and Pepin JL. Obstructive sleep apnoea syndrome. *Nat Rev Dis Primers* **1**: 15015, 2015.
15. Levy P, Pepin JL, Deschaux-Blanc C, Paramelle B, and Brambilla C. Accuracy of oximetry for detection of respiratory disturbances in sleep apnea syndrome. *Chest* **109**: 395-399, 1996.
16. Martin MS, Sforza E, Roche F, Barthelemy JC, and Thomas-Anterion C. Sleep breathing disorders and cognitive function in the elderly: an 8-year follow-up study. the proof-synapse cohort. *Sleep* **38**: 179-187, 2015.
17. Metzen E, Wolff M, Fandrey J, and Jelkmann W. Pericellular PO2 and O2 consumption in monolayer cell cultures. *Respir Physiol* **100**: 101-106, 1995.
18. Murphy AM, Thomas A, Crinion SJ, Kent BD, Tambuwala MM, Fabre A, Pepin JL, Roche HM, Arnaud C, and Ryan S. Intermittent hypoxia in obstructive sleep apnoea mediates insulin resistance through adipose tissue inflammation. *Eur Respir J* **49**, 2017.
19. Nieto FJ, Peppard PE, Young T, Finn L, Hla KM, and Farre R. Sleep-disordered breathing and cancer mortality: results from the Wisconsin Sleep Cohort Study. *Am J Respir Crit Care Med* **186**: 190-194, 2012.
20. Otto CM and Baumgardner JE. Effect of culture PO2 on macrophage (RAW 264.7) nitric oxide production. *Am J Physiol Cell Physiol* **280**: C280-287, 2001.
21. Pavlikova N, Weiszenstein M, Pala J, Halada P, Seda O, Elkalaf M, Trnka J, Kovar J, and Polak J. The effect of cultureware surfaces on functional and structural components of differentiated 3T3-L1 preadipocytes. *Cell Mol Biol Lett* **20**: 919-936, 2015.
22. Polak J, Studer-Rabeler K, McHugh H, Hussain MA, and Shimoda LA. System for exposing cultured cells to intermittent hypoxia utilizing gas permeable cultureware. *Gen Physiol Biophys* **34**: 235-247, 2015.
23. Polotsky VY, Savransky V, Bevans-Fonti S, Reinke C, Li J, Grigoryev DN, and Shimoda LA. Intermittent and sustained hypoxia induce a similar gene expression profile in human aortic endothelial cells. *Physiol Genomics* **41**: 306-314, 2010.
24. Ryan S, Taylor CT, and McNicholas WT. Selective activation of inflammatory pathways by intermittent hypoxia in obstructive sleep apnea syndrome. *Circulation* **112**: 2660-2667, 2005.
25. Sorg BS, Hardee ME, Agarwal N, Moeller BJ, and Dewhirst MW. Spectral imaging facilitates visualization and measurements of unstable and abnormal microvascular oxygen transport in tumors. *J Biomed Opt* **13**: 014026, 2008.
26. Tamisier R, Briançon-Marjollet A, Levy P, and Pepin JL. Animal and physiological settings of IH exposure. In: *ERS Monograph: Obstructive Sleep Apnea*, 2015, p. 1-8.
27. Taylor CT, Kent BD, Crinion SJ, McNicholas WT, and Ryan S. Human adipocytes are highly sensitive to intermittent hypoxia induced NF-kappaB activity and subsequent inflammatory gene expression. *Biochem Biophys Res Commun* **447**: 660-665, 2014.
28. Toffoli S, Delaive E, Dieu M, Feron O, Raes M, and Michiels C. NDRG1 and CRK-I/II are regulators of endothelial cell migration under Intermittent Hypoxia. *Angiogenesis* **12**: 339-354, 2009.
29. Toffoli S, Roegiers A, Feron O, Van Steenbrugge M, Ninane N, Raes M, and Michiels C. Intermittent hypoxia is an angiogenic inducer for endothelial cells: role of HIF-1. *Angiogenesis* **12**: 47-67, 2009.
30. Wang ZF, Kang J, and Dai B. [Expression and activation of hypoxia inducible factor-1alpha and iNOS in the brain of rats with chronic intermittent hypoxia]. *Zhonghua Jie He He Hu Xi Za Zhi* **32**: 739-743, 2009.
31. Yuan G, Nanduri J, Bhasker CR, Semenza GL, and Prabhakar NR. Ca2+/calmodulin kinase-dependent activation of hypoxia inducible factor 1 transcriptional activity in cells subjected to intermittent hypoxia. *J Biol Chem* **280**: 4321-4328, 2005.

Table 1.

Gas settings and duration (in seconds or minutes) of the normoxic and hypoxic phases of the various protocols tested. In all the protocols except for 2% 30"-30" and 2% 1'-1', a 20% O_2 normoxic burst was used before stabilization at 16% O_2 in order to decrease the duration of the ascending phase. Similarly, in 5% O_2 protocols, a 3% O_2 hypoxic burst was used before stabilization at 5% O_2 in order to decrease the duration of the descending phase.

Protocol	20%	16%	3%	5%	2%
2% 30”-30”	0.5				0.5
2% 1’-1’	1				1
2% 2’-2’	1	1			2
2% 3’-3’	1	2			3
2% 3’-5’	1	2			5
2% 5’-5’	1	4			5
5% 2’-2’	1	1	1	1	
5% 3’-3’	1	2	1	2	

Table 2.

Nadir and peak pO_2 values and cycle amplitude (calculated delta value) measured in 55-mm dishes submitted to the intermittent hypoxia protocols depicted in *Table 1*. Data (in mmHg) are means ± SEM. * $P < 0.05$ and ** $P < 0.01$ vs. 2% 5’-5’ protocol, two-way ANOVA. p=0.08 for Delta 2% 2'-2' vs 2% 5'-5'.

Protocol	Nadir	Peak	Delta
2% 30”-30”	58.5 ± 2.2 **	105.8 ± 1.3 **	47.3 ± 3.0 **
2% 1’-1’	44.3 ± 1.5 **	124.3 ± 2.4	79.9 ± 3.6 *
2% 2’-2’	33.8 ± 0.3	118.2 ± 2.4	84.4 ± 1.9
2% 3’-3’	30.3 ± 1.4	115.4 ± 4.4	85.1 ± 3.7
2% 3’-5’	24.9 ± 2.0	120.4 ± 4.5	95.5 ± 3.3
2% 5’-5’	25.5 ± 1.2	120.6 ± 1.9	95.1 ± 1.6
5% 2’-2’	38.0 ± 3.1 *	123.3 ± 3.3	85.3 ± 6.4
5% 3’-3’	39.7 ± 5.5 *	126.0 ± 8.0	86.3 ± 4.5

Table 3.

Impact of culture medium volume on intermittent hypoxia cycles. Nadir and peak pO_2 values and cycle amplitude (calculated delta value) measured in 55-mm dishes filled with different volumes of culture medium and submitted to protocol 2% 5'-5'. Data (in mmHg) are means ± SEM. *n* = 3 independent experiments. Medium volume significantly alters the cycles (*P* = 0.037, two-way ANOVA). * *P* = 0.019 vs. nadir at 5ml, two-way ANOVA. p=0.07 for nadir 3mL vs 7mL, p=0.06 for peak 3mL vs 5mL.

Volume	Nadir	Peak	Delta
3 ml	36.7 ± 2.9 *	138.0 ± 0.1	101.3 ± 2.9
5 ml	27.2 ± 2.4	130.3 ± 0.9	103.2 ± 1.6
7 ml	29.3 ± 3.0	134.0 ± 3.1	104.7 ± 0.3

Table 4.

Impact of the presence of cells on intermittent hypoxia cycles. Nadir and peak pO_2 values and cycle amplitude (calculated delta value) measured in 55-mm dishes filled with 4ml of culture medium with or without a confluent layer of 4T1 cells, and exposed to protocol 2% 5'-5'. The presence of cells does not change nadir values but lowers peak and delta values. Data (in mmHg) are means ± SEM. *n* = 3 independent experiments performed in duplicates. ** *P* < 0.01 vs. corresponding values without cells, two-way ANOVA.

	Nadir	Peak	Delta
Without cells	28.8 ± 2.4	124.4 ± 0.9	95.6 ± 2.9
With cells	26.7 ± 2.7	113.1 ± 3.5 **	86.5 ± 1.5 **

Figure legends

Fig. 1.

Pictures showing the holders for 55-mm dishes (first lane) and for 24-well and 96-well plates (second lane). The dishes or plates are maintained with forceps in order to avoid air leakage.

Fig. 2.

Characterization of pO_2 cycles at the membrane level in 55-mm dishes containing 5ml of culture medium without cells. *A-F* show typical cycles measured with the following intermittent hypoxia protocols: 2% 30"-30" *(A)*, 2% 1'-1' *(B)*, 2% 2'-2' *(C)*, 5% 2'-2' *(D)*, 2% 3'-3' *(E)* and 2% 5'-5' *(F)*. *G* shows peak and nadir pO_2 values and amplitude of pO_2 variation for each protocol. Data are from at least 3 independent measurements and for over 10 independent experiments for protocol 2% 5'-5'. *H* shows cycles measured in three 55-mm dishes exposed simultaneously in holder to protocol 5% 2'-2'.

Fig. 3.

Characterization of pO_2 cycles in 24-well plates. *A*: Typical cycles measured at the membrane level in 24-well plates (filled with 500 µl PBS) with protocol 2% 5'-5'. Cycles measured in 96-well plates were similar. *B*: Typical measurements in 3 plate holders serially connected (protocol 2% 5'-5'), nadir and peak pO_2 values and cycle amplitude (calculated delta value) for the 3 consecutive plate holders. Cycles were only very slightly attenuated, with no significant difference. *C*: Nadir and peak pO_2 values and cycle amplitude (calculated delta value) in gas-permeable 24-well plates with 50 µm-thick (Sarstedt) or 25 µm-thick (Zell-kontakt) membranes using protocol 2% 5'-5'. *n* = at least 5 independent measurements. ** $P < 0.01$ for nadir and cycle amplitude vs. 25 µm-thick membranes, Mann-Whitney rank sum tests.

Fig. 4.

582 Evolution of the cycles throughout the culture medium and in transwells. *A*: Typical nadir
583 and peak pO_2 values and cycle amplitude (calculated delta value) at different heights above
584 the membrane. Measurements were performed with protocol 2% 5'-5' in 55-mm dishes.
585 Similar results were observed in 96-well dishes. Data (in mmHg) are means ± SEM. *n* = at
586 least 3 independent experiments. *B*: Cycle amplitude (calculated delta value) at different
587 heights above the membrane in unsealed and sealed 55-mm dishes, and corresponding
588 calculated Area Under the Curve (AUC). Measurements were performed with protocols 2%
589 3'-3' (diamonds) and 2% 5'-5' (squares) in unsealed dishes and with protocol 2% 5'-5'
590 (triangles) in dishes sealed with tape to limit gas exchanges with incubator air. Data are
591 means ± SEM. *n* = at least 3 independent experiments. * Area under the curve vs. protocol
592 2% 3'-3' in unsealed dishes, $P = 0.012$ (one-way ANOVA). There was no significant difference
593 in cycle amplitude between unsealed and sealed plates at membrane level (probe height =
594 0). *C*: Cycles measured with protocol 2% 5'-5' inside a 8µm-pore transwell with 100 µl of
595 medium placed in a 24-well plate (Zell-kontakt) filled with 600 µL of culture medium.
596
597 **Fig. 5.**
598 Comparison of pO_2 values in standard and permeable dishes under normoxia. pO_2 values
599 were measured at the level of the cell layer in standard plastic or gas-permeable 55-mm
600 dishes plated with HAoEC or 4T1 cells at different cell confluences and incubated under
601 normoxia. Cultures were pre-equilibrated at 21% O_2 in a standard incubator, placed under
602 normoxia (21% O_2 + 5% CO_2) in the intermittent hypoxia device and allowed to equilibrate
603 for at least 30 minutes before pO_2 measurements. Individual data and median are plotted,
604 *n*=5 measurements from 3 independent experiments. * $P < 0.05$ and ** $P < 0.01$ vs. gas
605 permeable plates, Mann-Whitney rank sum test. p=0.09 for HAoEC cells, permeable vs
606 plastic dish.
607
608 **Fig. 6.**
609 Intermittent hypoxia increases HIF-1α expression. *A*: Expression of HIF-1α in HAoEC and 4T1
610 cells after 6 hours of exposure to protocol 2% 5'-5', expressed as a ratio of HIF-1α expression
611 in cells exposed to 6 hours of normoxia (16% O_2). * $P < 0.05$ vs. normoxia, Mann-Whitney
612 rank sum test. *B*: Expression of HIF-1α in a blood brain barrier model composed of b. End3
613 endothelial cells and C6 astrocytes after 24 hours of IH (2h of 2% 5'-5' and 6h of normoxia,

repeated 3 times). Individual data and median are plotted. n = 3 independent experiments, ** $P < 0.01$ vs. normoxia, Mann-Whitney rank sum test.

Fig. 1

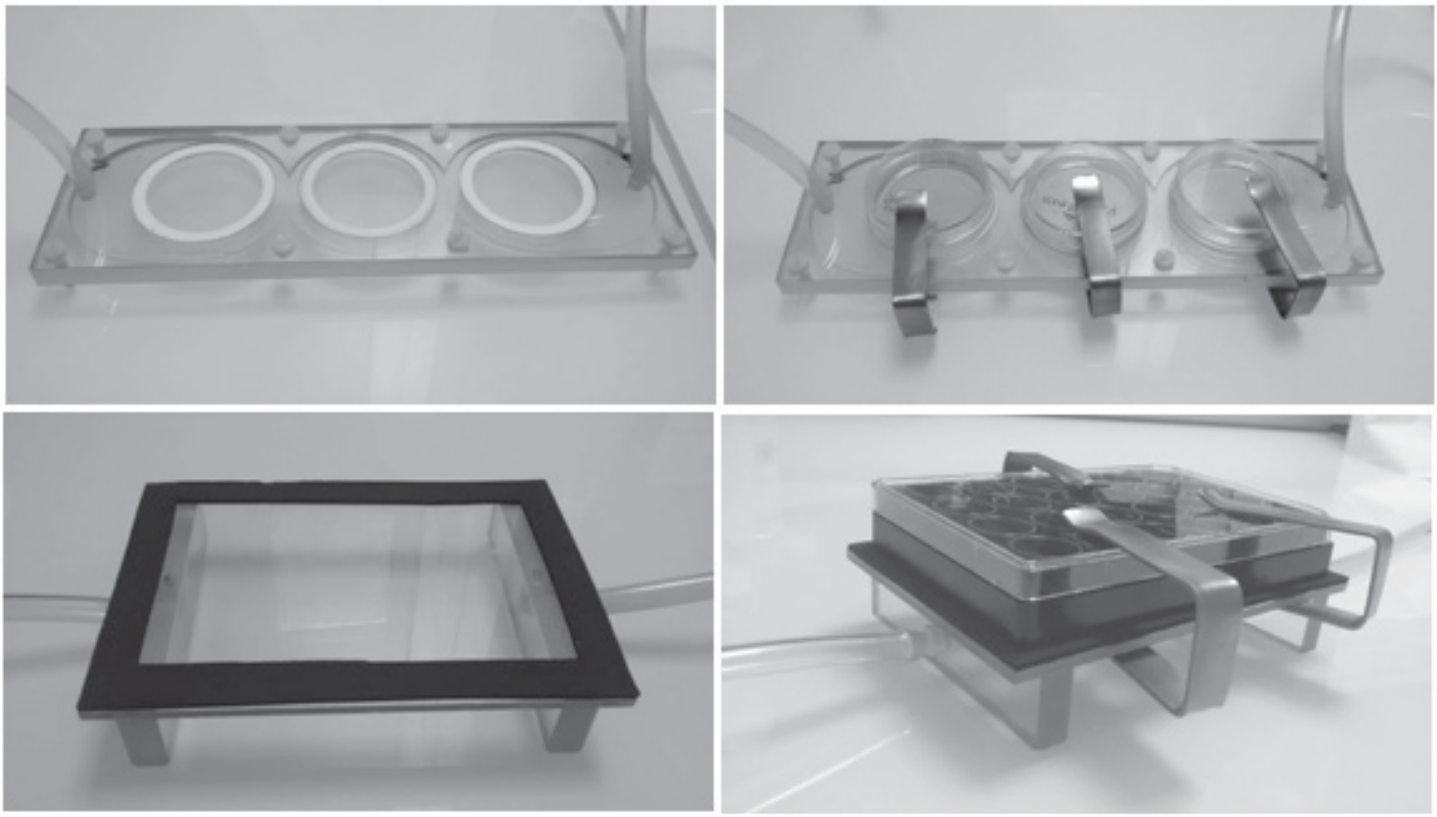

Fig. 2

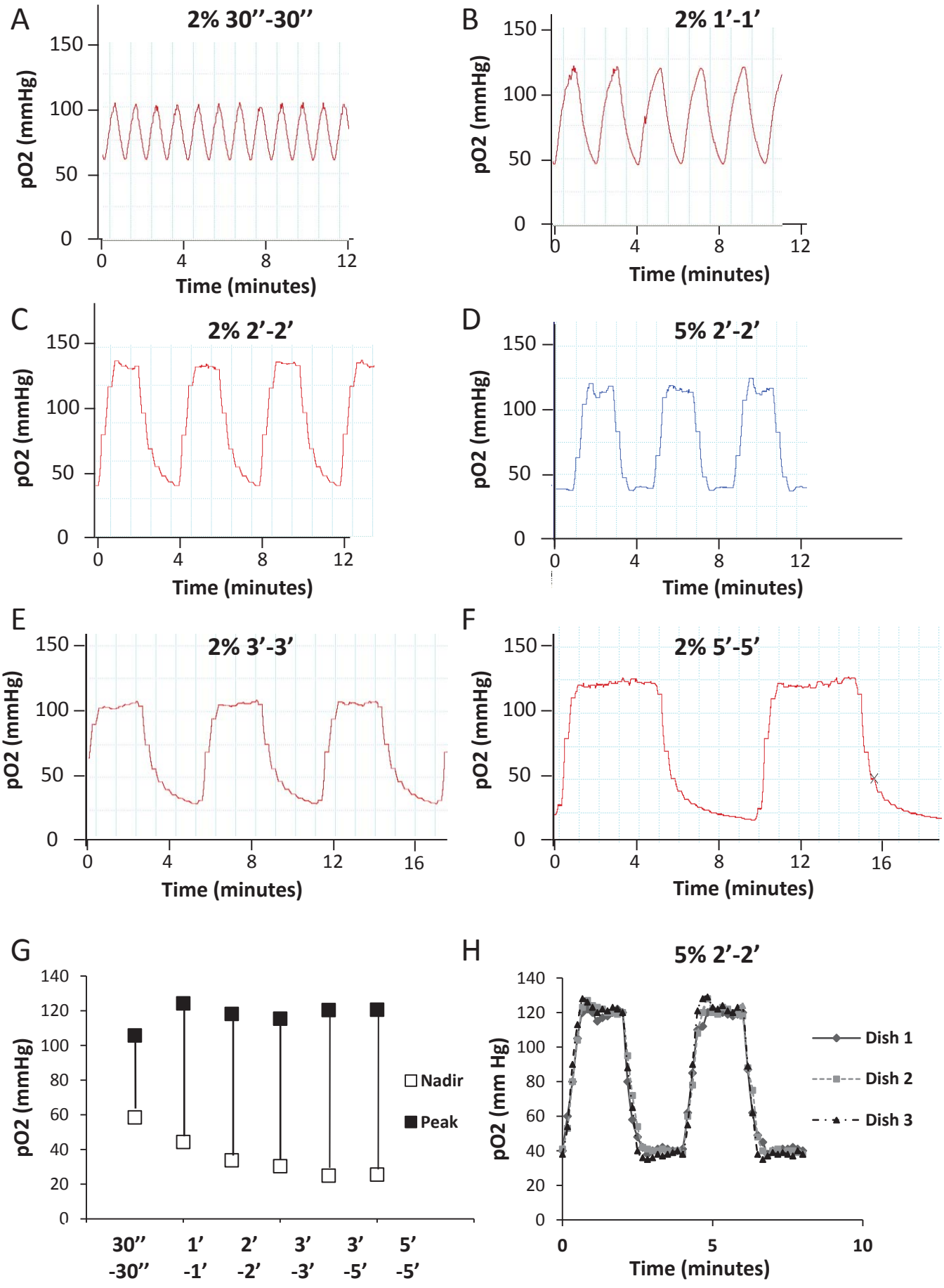
A
2% 30''-30''
pO2 (mmHg)
Time (minutes)
B
2% 1'-1'
pO2 (mmHg)
Time (minutes)
C
2% 2'-2'
pO2 (mmHg)
Time (minutes)
D
5% 2'-2'
pO2 (mmHg)
Time (minutes)
E
2% 3'-3'
pO2 (mmHg)
Time (minutes)
F
2% 5'-5'
pO2 (mmHg)
Time (minutes)
G
pO2 (mmHg)
Nadir
Peak
30'' -30''
1' -1'
2' -2'
3' -3'
3' -5'
5' -5'
H
5% 2'-2'
pO2 (mm Hg)
Time (minutes)
Dish 1
Dish 2
Dish 3

Fig. 3

A

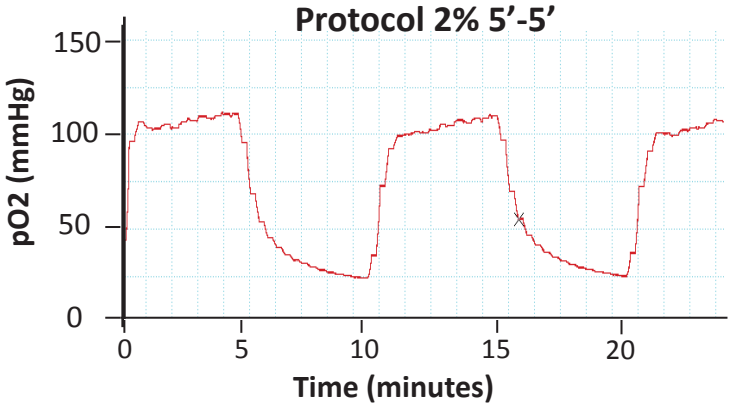

B

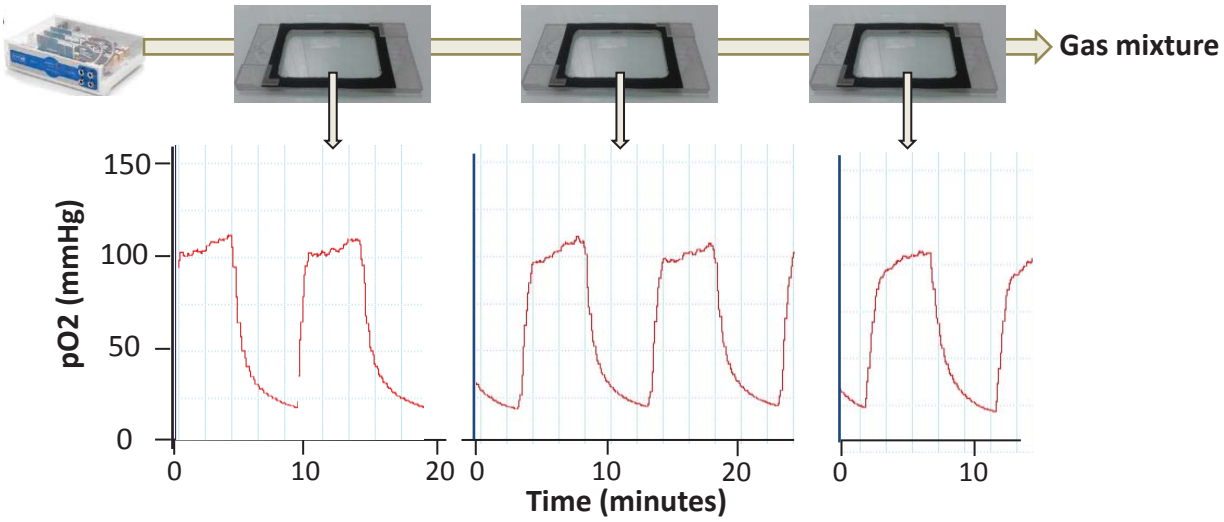

	Nadir	Peak	Delta
First plate	27.0 ± 1.9	118.8 ± 3.6	91.8 ± 2.9
Second plate	26.3 ± 3.2	118.7 ± 6.4	92.3 ± 3.5
Third plate	30.7 ± 4.3	122.7 ± 8.1	92.0 ± 4.4

C

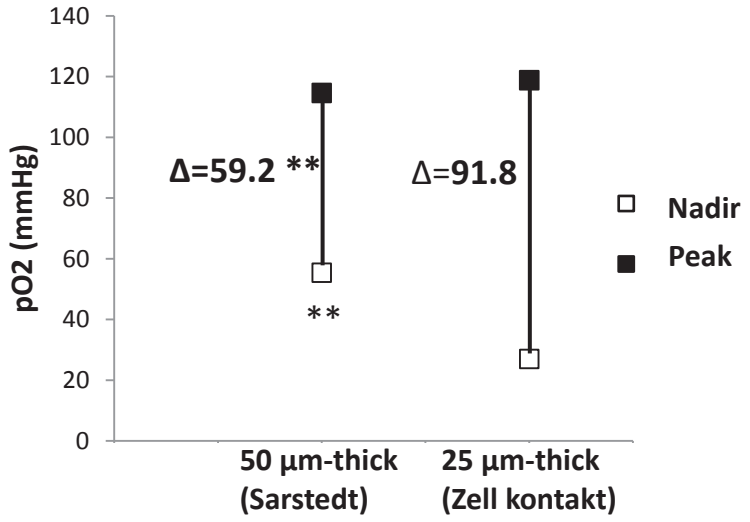

Fig. 4

A

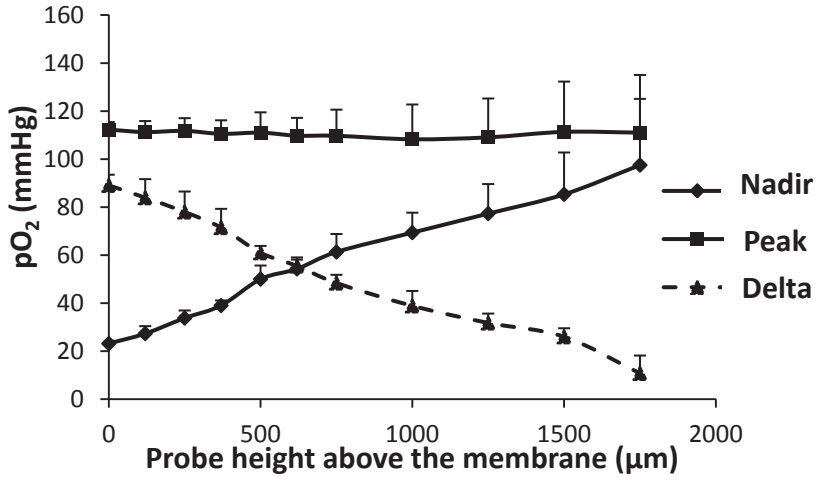
160
140
120
100
80
60
40
20
0
pO2 (mmHg)
0
500
1000
1500
2000
Probe height above the membrane (µm)
Nadir
Peak
Delta

B

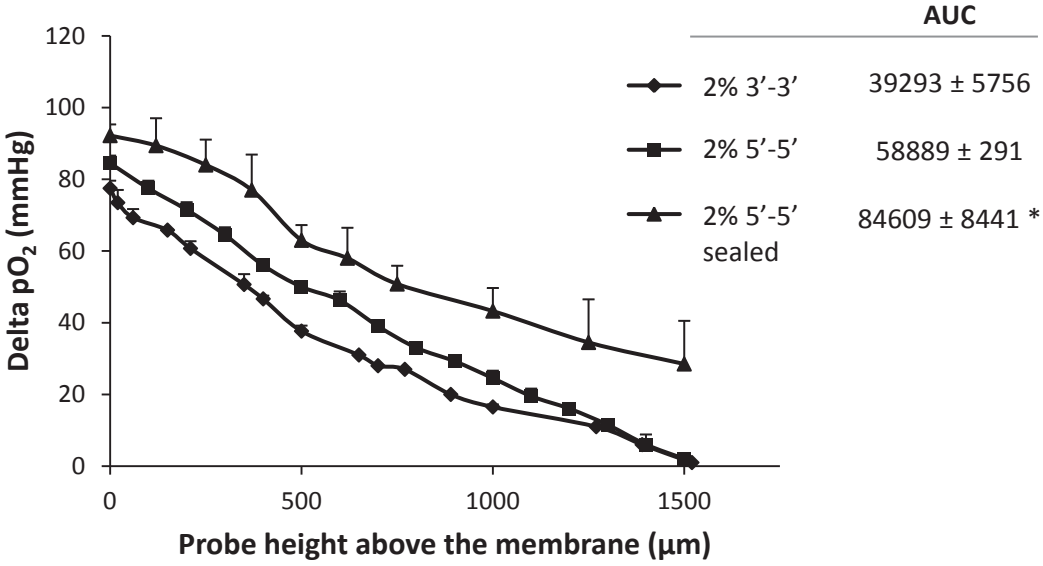
120
100
80
60
40
20
0
Delta pO2 (mmHg)
0
500
1000
1500
Probe height above the membrane (µm)
AUC
2% 3'-3'
39293 ± 5756
2% 5'-5'
58889 ± 291
2% 5'-5' sealed
84609 ± 8441 *

C

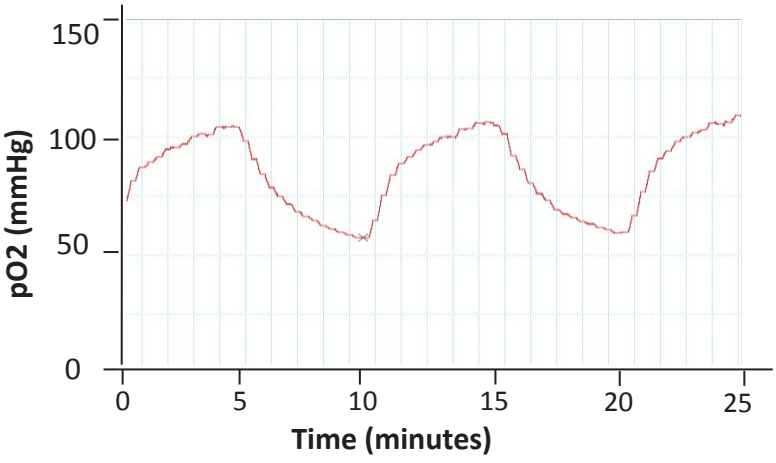
150
100
50
0
pO2 (mmHg)
0
5
10
15
20
25
Time (minutes)

Fig. 5

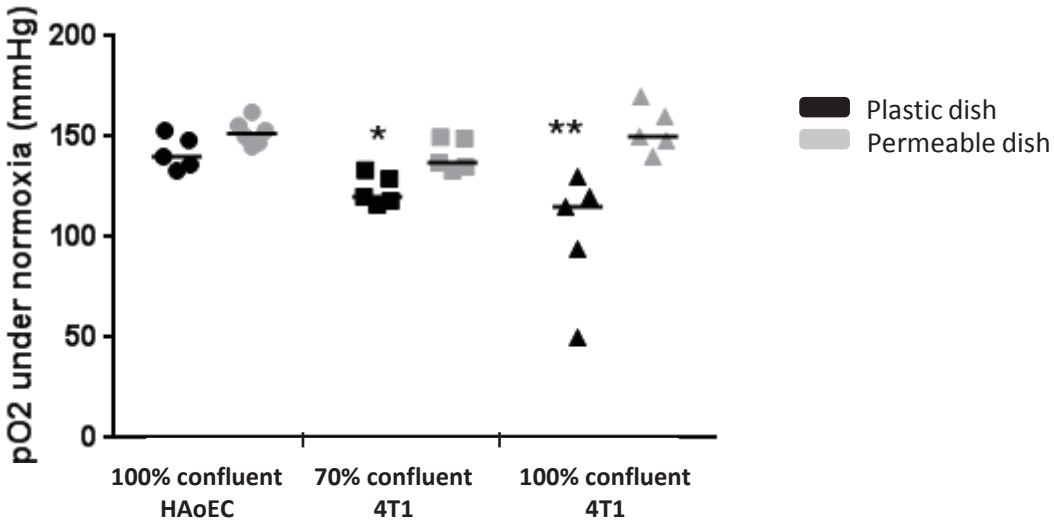
pO2 under normoxia (mmHg)
200
150
100
50
0
*
**
100% confluent HAoEC
70% confluent 4T1
100% confluent 4T1
Plastic dish
Permeable dish

Fig. 6

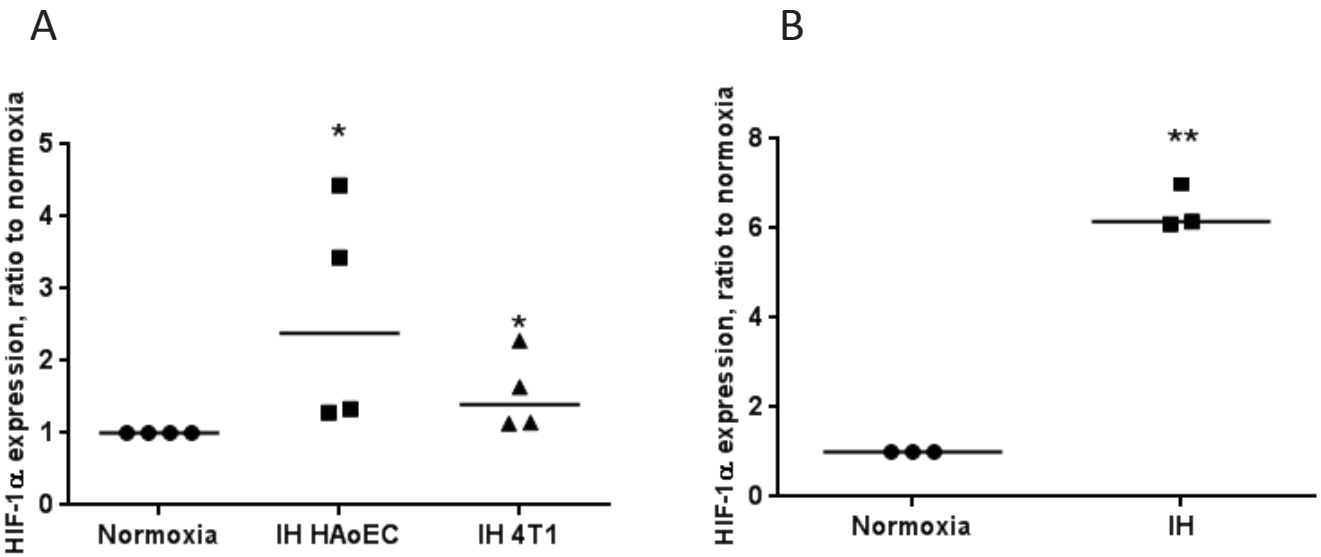
A
B
HIF-1α expression, ratio to normoxia
0
1
2
3
4
5
*
*
Normoxia
IH HAoEC
IH 4T1
HIF-1α expression, ratio to normoxia
0
2
4
6
8
**
Normoxia
IH